Experimental Study of Drying/Evaporation in an Effective 2-D Porous Medium

A.G. Yiotis*, I.N. Tsimpanogiannis** and A. K. Stubos***

* Environmental Research Laboratory, National Center for Scientific Research "Demokritos", 15310 Aghia Paraskevi, Greece, yiotis@ipta.demokritos.gr
** Environmental Research Laboratory, National Center for Scientific Research "Demokritos", 15310 Aghia Paraskevi, Greece, tsimpano@usc.edu
*** Environmental Research Laboratory, National Center for Scientific Research "Demokritos", 15310 Aghia Paraskevi, Greece, stubos@ipta.demokritos.gr

ABSTRACT

We perform drying/evaporation experiments in 2-D effective porous media (Hele-Shaw cells packed with glass microspheres) in order to understand how the mechanisms occurring at the pore level affect the process at the continuum level. We study the receding of the gas/liquid front inside the porous medium. The drying/evaporation front is a fractal object with finite width that obeys a power-law scaling with a diffusion-based capillary number. We calculate the fractal dimension of the front (D_e=1.36±0.08), which is in very good agreement with reported theoretical and experimental values). The exponent of the power-law scaling is obtained through the experiments and is in good agreement with the theoretical value (-0.57 in 2-D and -0.47 in 3-D). Finally, we obtain the drying curve for the porous medium. The typical drying periods are identified.

Keywords: evaporation, experimental, percolation, Hele-Shaw cell, scaling

1 INTRODUCTION

Liquid-to-gas phase change, where the mass transfer that drives the process occurs in the gas phase, and the subsequent growth of the produced gas phase within a porous medium, is involved in a wide variety of processes of significant scientific and industrial interest. The process has applications in the energy production area (e.g. light oil recovery from fractured reservoirs by lean-gas injection [1]), the environmental protection area (e.g. soil remediation by air sparging or similar techniques [2]), as well as other industrial or health-related applications. This particular phase-change process, also known as evaporation or drying (depending on the application field used) has a plethora of practical applications including among others in food industry, pharmaceuticals, ceramics, cements and other construction materials, paper and textile industry, and fuel cells. Evaporation is also one of the dominant processes (another one being the capillarity-driven liquid flow) in microfluidic devices that are used to cool electronic equipment with applications ranging from satellites to portable electronics.

For the drying/evaporation process significant progress has been achieved in our understanding of the various phenomena occurring at the pore/pore-network scale including the effects of capillary [3], viscous [4, 5], and gravity forces [6, 7], convective transfer [4], counter-current diffusion in both gas and liquid phase, and film flows [8, 9].

In addition to extensive numerical simulation studies, visualization experiments using transparent 2-D porous media (e.g. glass or PMMA micromodels, Hele-Shaw cells) have contributed significantly in identifying mechanisms at the pore level. Such mechanisms were subsequently incorporated in pore network models resulting, thus, in more accurate representation of the physics at the pore level.

In this study we report experimental results using Hele-Shaw cells packed with glass microspheres. Processes of interest to this study included the isothermal drying and evaporation inside porous media.

2 EXPERIMENTS

In this study experiments of drying in 2-D effective microporous media were conducted. In particular, Hele-Shaw cells packed with borosilicate glass microspheres (40 μm, 140 μm in diameter) were constructed. Two pieces of glass plates (with dimensions 2.35 cm × 1.65 cm) were put together with epoxy glue (three sides were glued, while the fourth remained open to the environment). The constructed cells had a gap of 550 μm (z-direction) rendering the porous medium essentially 2-D. Given the x-, y-, z-, dimensions of the cells we estimate that each cell had approximately 580 × 410 × 13 (for cells packed with spheres having diameter 40 μm) or 160 × 110 × 3 (for cells packed with spheres having diameter 140 μm) layers of glass microspheres. The cells had an estimated porosity in the range of 31-35%.

The cells were saturated with liquid hexane. The following parameter values are applicable: interfacial tension γ=19×10^{-3} N/m, liquid phase density ρ_l=650 kg/m^3,

gas phase density ρ_g=4.4 kg/m^3, equilibrium concentration C_e=0.266 kg/m^3 and binary diffusion coefficient of hexane into air D=6.38×10^{-6} m^2/s.

Initially the cells were saturated with hexane and subsequently the glass microspheres were introduced carefully in order to prevent air from being trapped in the cell. Finally, the cells were positioned horizontally in order to study the evolution of the liquid/gas interface as it receded within the porous medium. Experiments were conducted at ambient conditions. Figure 1 shows a schematic of the experimental setup used in this study. The experiments were recorded with a CCD camera and stored for additional studies. Typical examples of experimental images depicting the evolution of the evaporation process at two different times are shown in Figures 2a, 2b. After the images were captured an image processing procedure was applied to them (Figure 2c, 2d). From this procedure we extracted information that delineates the motion of the gas/liquid interface as a function of time.

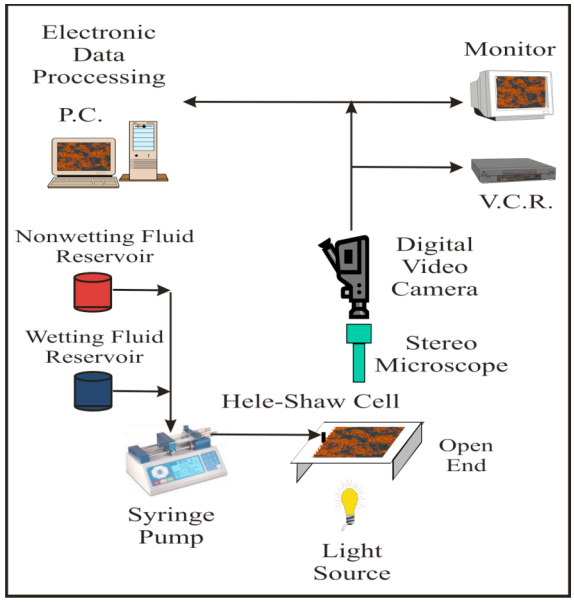

Figure 1: Schematic of the experimental setup.

3 RESULTS AND DISCUSSION

3.1 Fractal Dimension of the Drying/ Evaporation Front

Shaw [10] was the first to identify the evaporation process as an immiscible displacement where essentially a less viscous fluid (gas phase) displaces a more viscous fluid (liquid phase), while a liquid counter flow through liquid films occurs in the gas-phase-dominated part of the porous medium. Immiscible displacement processes have been successfully simulated with Invasion Percolation Theory. Of interest is the external perimeter of the invasion percolation cluster. For the case of drying this corresponds to the drying front. Essentially it includes all the liquid–occupied pores at the perimeter that have a gas–occupied pore as a next–nearing neighbor.

Using the processed images we could extract the gas/liquid interface (i.e. location within the medium and shape of the interface). The mass fractal dimension of the gas/liquid interface, then, was measured from the obtained images, with the "box-counting" method (Mandelbrot [11], Feder [12]). In this approach the fractal set is completely covered by non–overlapping boxes of Eucledean size δ. The number $N(\delta)$ of such boxes required is plotted and the following relation is used in the limit $\delta \to 0$.

$$N(\delta) \propto \delta^{-D_e} \tag{1}$$

The mass fractal dimension was found to be equal to D_e=1.36±0.08. The current experimental value is in very good agreement with the experimental results of Shaw [10] who reported that the mass fractal dimension of the drying front is equal to 1.38±0.02. The obtained value in this study is also in good agreement with the immiscible displacement (drainage) results obtained from the experiments (1.34±0.04) and numerical simulations (1.39±0.02) of Birovljev et al. [13].

3.2 Scaling of the Width of the Evaporation Front

As the evaporation/drying process advances inside the porous medium, the frontal region (i.e. the gas/liquid interface that separates the dry and wet regions) is a fractal object that has a finite width σ_f.

Tsimpanogiannis et al. [14] performed a detailed scaling analysis of the front width and demonstrated that it scales with a diffusion-based, dimensionless, capillary number, Ca_D, or the velocity of the front, u_f as:

$$\sigma_f \propto Ca_D^{-\nu/(\nu+1)} \propto u_f^{-\nu/(\nu+1)} \tag{2}$$

where ν is the correlation length exponent of percolation, with values ν=4/3 in 2-D and ν=0.88 in 3-D (Stauffer and Aharony [15]). Therefore, the theoretical predictions for the exponent $-\nu/(\nu+1)$ are equal to –0.57 for 2-D and –0.47 for 3-D. This capillary number reflects the fact that drying is controlled by diffusion in the gas phase in contrast to external immiscible displacement. In principle, when a less viscous fluid displaces a more viscous fluid, unstable patterns of viscous fingering result. However, the drying front is a stable front with a finite width.

As a result of the self–affinity of the front it is useful to define the drying mean–front position, x_f, as follows for the case of 2-D (see also the detailed discussion by Gouyet et al. [16] for the case of 3-D diffusion fronts):

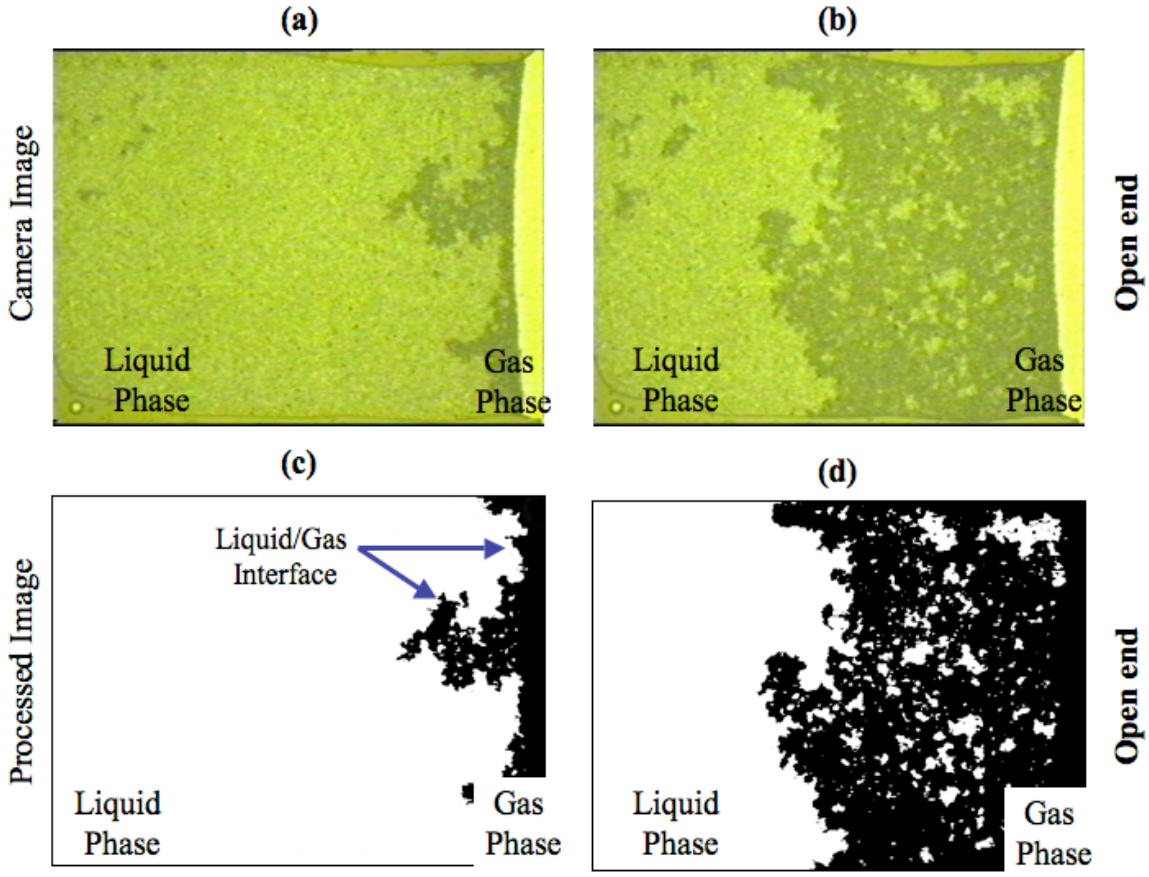

Figure 2: Camera images from the Hele-Shaw cell at different evaporation times: **a)** 4 minutes of evaporation, **b)** 30 minutes of evaporation. The corresponding processed images: **c)** 4 minutes of evaporation, **d)** 30 minutes of evaporation. (Gas phase is depicted in black and liquid phase in white).

$$x_f = \frac{\int_0^\infty x \cdot p_f(x)dx}{\int_0^\infty p_f(x)dx} \tag{3}$$

where $p_f(x)$ is the probability to find a pore of the interface at x. The mean–front position and the width of the front are related through:

$$\sigma_f^2 = \frac{\int_0^\infty (x - x_f)^2 \cdot p_f(x)dx}{\int_0^\infty p_f(x)dx} \tag{4}$$

We calculated the gas/liquid front width (σ_f) from the experiments. Figure 3 shows the front width as a function of the velocity of the interface. A power-law scaling relation of the front width with the velocity of the interface (u_f) or a diffusion-based capillary number (Ca_D) is obtained, given as:

$$\sigma_f \propto Ca_D^{-0.58} \propto u_f^{-0.58} \tag{5}$$

The scaling exponent calculated from the experiments performed during this study is in very good agreement with the theoretical value for 2-D reported by Tsimpanogiannis et al. [14].

Shaw [10] also measured the width of the gas/liquid interface (drying front) as a function of the velocity in similar experiments. He used a random packing of 0.5-μm-diameter silica spheres packed in a 2.5 cm × 4.0 cm × 15-20 μm glass cell. Based on the thickness of the cell we estimate that approximately 30-40 micro-sphere layers were on the z-direction (compare with the 3-13 of this study). Shaw reported a scaling exponent equal to -0.47, which is closer to the theoretical value for 3-D. Note, however, that for the case of 3-D the scaling exponent was developed for the front tail width [16], where the pattern is fractal, which may not be the same quantity measured experimentally by Shaw [10].

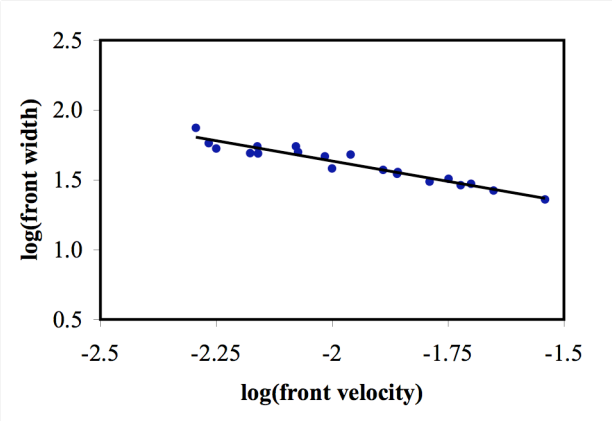

Figure 3: Log-log plot of the front width (σ_f) as a function of the front velocity (u_f). The solid line is the best-fit line and has a slope equal to -0.58.

A more extended experimental study is required to clarify the issue of the scaling of the evaporation front.

3.3 Drying Rate Curve

An experiment was also performed during which the weight of the packed cell was monitored as a function of time. As a result the drying rate curve could be obtained. This result is shown in Figure 4. The drying curve has the typical form discussed by Yiotis et al. [7]. We can observe the characteristic drying periods. In particular, we can clearly observe in the figure the initial drying period, the constant rate period (CRP), and the falling rate period (FRP). A fourth period that is not clearly shown in the figure is the receding front period (see the detailed discussion in [7]).

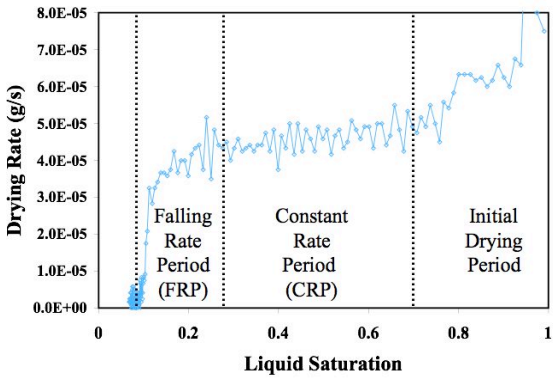

Figure 4: Drying rate curve at ambient conditions for a Hele-Shaw cell packed with glass microspheres (140 μm diameter) and saturated with hexane.

4. CONCLUSIONS

We performed evaporation/drying experiments in 2-D Hele-Shaw cells packed with glass microspheres and saturated with hexane. We examined the receding of the gas/liquid front inside the porous medium. The fractal dimension of the front and the exponent of the power-law describing the front width were calculated from the experiments. Both were found to be in very good agreement with previously reported theoretical and experimental values. Finally, the drying curve for the porous medium was obtained which exhibited the characteristic drying periods.

REFERENCES

[1] I.N. Tsimpanogiannis, A.K. Stubos, Y.C. Yortsos, Ind. Eng. Chem. Res., 39, 1505, 2000.
[2] C.K. Ho, K.S. Udell, Int. J. Heat Mass Transfer, 38, 339, 1995.
[3] M. Prat, Int. J. Multiphase Flow, 21, 875, 1995.
[4] A.G. Yiotis, A.K. Stubos, A.G. Boudouvis, Y.C. Yortsos, Adv. Water Res., 24, 439, 2001.
[5] M. Prat, F. Bouleux, Phys. Rev. E, 60, 5647, 1999.
[6] J.B. Laurindo, M. Prat, Chem. Eng. Sci., 51, 5171, 1996.
[7] A.G. Yiotis, I.N. Tsimpanogiannis, A.K. Stubos, Y.C. Yortsos, J. Colloid Interface Sci., 297, 738, 2006.
[8] A.G. Yiotis, A.K. Stubos, A.G. Boudouvis, I.N. Tsimpanogiannis, Y.C. Yortsos, AIChE J., 50, 2721, 2003.
[9] M. Prat, Int. J. Heat Mass Transfer, 50, 1455, 2007.
[10] T.M. Shaw, Phys. Rev. Lett., 59, 1671, 1987.
[11] B.B. Mandelbrot, "The Fractal geometry of Nature", Freeman & Co, New York, 1982.
[12] J. Feder, "Fractals", Plenum Press, New York, 1988.
[13] A. Birovljev, L. Furuberg, J. Feder, T. Jossang, K.J. Maloy, A. Aharony, Phys. Rev. Lett., 64, 584, 1991.
[14] I.N. Tsimpanogiannis, Y.C. Yortsos, S. Poulou, N. Kanellopoulos, A.K. Stubos, Phys. Rev. E, 59, 4353, 1999.
[15] D. Stauffer, A. Aharony, "Introduction to Percolation Theory", Taylor & Francis, London, 1994.
[16] J.-F. Gouyet, M. Rosso, B. Sapoval, Phys. Rev. B, 37, 2838, 1988.